This is the peer-reviewed, final accepted version for American Mineralogist, published by the Mineralogical Society of America.
The published version is subject to change. Cite as Authors (Year) Title. American Mineralogist, in press.
DOI: https://doi.org/10.2138/am-2022-8254. http://www.minsocam.org/

Contamination of heterogeneous lower crust in Hannuoba tholeiite: evidence from in situ trace elements and strontium isotopes of plagioclase Word Count:6669 Revision 1

Yu-Tong Su[1,2,3] Zong-Feng Yang [1,2,4] ✉ Shuang-Yan Guo[1] Pei-Pei Li[1,2,4]

1 School of Earth Sciences and Resources, China University of Geosciences, Beijing, 100083, China

2 State Key Laboratory of Geological Processes and Mineral Resources, China University of Geosciences, Beijing, 100083, China

3 Now at School of Earth and Space Sciences, Peking University, Beijing, 100871, China

4 Research Center of Genetic Mineralogy, China University of Geosciences, Beijing, 100083, China

Abstract

The Hannuoba basalt, located in the northern margin of the North China Craton, is a typical intracontinental basalt with ocean island basalt-like geochemical features and has been extensively studied. However, its origin and deep processes, such as magma mixing and crystallization conditions, are still unclear. To further understand the mechanisms leading to the compositional heterogeneity and magmatic processes of Hannuoba basalt at crustal and/or mantle depth, in-situ major element, trace element, and $^{87}Sr/^{86}Sr$ compositional heterogeneity of four representative plagioclase crystals in three Hannuoba tholeiite samples, as well as whole-rock major and trace elements data, are reported. According to the petrographic characteristics, the basalts

Always consult and cite the final, published document. See http:/www.minsocam.org or GeoscienceWorld

This is the peer-reviewed, final accepted version for American Mineralogist, published by the Mineralogical Society of America.
The published version is subject to change. Cite as Authors (Year) Title. American Mineralogist, in press.
DOI: https://doi.org/10.2138/am-2022-8254. http://www.minsocam.org/

are divided into fine-grained and coarse-grained groups. The anorthite content in plagioclase of samples varies in a small range (56-64%), but the content of trace elements in plagioclase from the coarse-grained samples is generally higher than that of the fine-grained samples. Clinopyroxene-melt equilibrium thermobarometer and plagioclase-clinopyroxene magnesium and rare earth element exchange thermometer show that the magma for the two types of basalt was stored and crystallized at a similar depth, and crystallized within a 20 ℃ (fine-grained basalt) and 50℃ (coarse-grained basalt) temperature window, which may be a reason for the grain size differences between the two types of basalts. We found that $^{87}Sr/^{86}Sr$ of all the studied plagioclase crystals varied from 0.70333 ± 0.00018 (2SE) to 0.70556 ± 0.00031 (2SE), a much large range than the whole rock of Hannuoba basalts reported previously and consistent with that of Cenozoic basalts in North China. Therefore, at least two kinds of melts with significant differences in isotope and minor heterogeneity in major and trace elements are injected into each magma plumbing system. The content of trace elements in the Hanuoba tholeiite is between the Hanuoba alkaline basalt and the lower crust, which can be explained by the mixing of the alkaline basalt and the lower crust, but the low $^{87}Sr/^{86}Sr$ (<0.704) characteristics of plagioclase cannot come from alkaline basalt, because trace element in the plagioclase is not in equilibrium with the alkaline basalt. Therefore, we believe that the compositional heterogeneity of Hannuoba tholeiitic basalt is mainly caused by the mixing of heterogeneous lower crust rather than different mantle-derived melts, which indicates the contribution of the continental lower crust to the continental basalt is more complicated than

Always consult and cite the final, published document. See http:/www.minsocam.org or GeoscienceWorld

This is the peer-reviewed, final accepted version for American Mineralogist, published by the Mineralogical Society of America.
The published version is subject to change. Cite as Authors (Year) Title. American Mineralogist, in press.
DOI: https://doi.org/10.2138/am-2022-8254. http://www.minsocam.org/

previously recognized.

Keywords: Basalt, plagioclase, strontium isotope, magmatic process, lower continental crust, Hannuoba

Introduction

A large number of studies show that the lower continental crust plays an important role in the geochemical diversity of continental basalts (Glazner et al., 1991; Jiang and Zhi, 2010; Liu et al., 2008b; Lustrino, 2005; Xu et al., 2017; Zeng et al., 2011). Many studies suggest that the signals of the lower continental crust imply that it is a source of material for basalt through the recycling of crustal materials. (Liu et al., 2008b; Xu et al., 2017; Zeng et al., 2011). Others, however have suggested that the contamination of the lower continental crust during the ascent of basaltic magma may be an important reason for the compositional diversity of continental basalts, but this contamination is usually very difficult to identify (Glazner and Farmer, 1992; Glazner et al., 1991; Jiang and Zhi, 2010) because the lower continental crust is mainly composed of mafic rocks with heterogeneous compositions (Rudnick and Fountain, 1995). Moreover, the heterogeneity becomes more significant through partial melting of the lower crust, crystallization differentiation, and mixing various mantle-derived magmas.

Always consult and cite the final, published document. See http:/www.minsocam.org or GeoscienceWorld

This is the peer-reviewed, final accepted version for American Mineralogist, published by the Mineralogical Society of America.
The published version is subject to change. Cite as Authors (Year) Title. American Mineralogist, in press.
DOI: https://doi.org/10.2138/am-2022-8254. http://www.minsocam.org/

Hannuoba basalt is a typical continental ocean island type basalt in that its rock types, petrography, and geochemistry have significant diversity. Although there is a long history of research, there is still controversy about how the lower continental crust affects the diversity of Hannuoba basalts (Basu et al., 1991; Guo et al., 2016; Jiang and Zhi, 2010; Liu et al., 1994; Qian et al., 2015; Song et al., 1990; Xu et al., 2017; Yang et al., 2016; Zhi et al., 1990). The systematic whole rock data of major and trace elements, as well as Sr, Nd, and Pb isotopes, seem to indicate that the ancient lithospheric mantle (Basu et al., 1991; Liu et al., 1994; Song et al., 1990) or recycled ancient oceanic crust and sediments (Qian et al., 2015; Xu et al., 2017) may be the source of Enrich Mantle I (EMI) end components in Hannuoba tholeiite. However, recent Os isotopic data show that the very high Os isotopic ratios, especially tholeiites, can only be explained by significant crustal contamination (Jiang and Zhi, 2010) rather than recycled products of the lower continental crust (Liu et al., 2008b). However, the details of crustal contamination are still unclear. One of the critical reasons may be that previous studies usually focus on the geochemical characteristics of the whole rock scale. The complex processes of crustal contamination and magmatic mixing are more commonly recorded in mineral growth zoning, but whole-rock compositions that average the signals of various minerals and glasses will weaken or eliminate the information recorded in minerals. Recent studies on melt inclusions in olivine have shown that melt inclusions with very heterogeneous isotopes but relatively homogeneous major and trace elements contribute to Hannuoba tholeiite (Qian et al., 2015). However, these melt inclusions probably only record a

Always consult and cite the final, published document. See http:/www.minsocam.org or GeoscienceWorld

This is the peer-reviewed, final accepted version for American Mineralogist, published by the Mineralogical Society of America.
The published version is subject to change. Cite as Authors (Year) Title. American Mineralogist, in press.
DOI: https://doi.org/10.2138/am-2022-8254. http://www.minsocam.org/

particular crystallization stage in the magma evolutionary history, and it may be homogenized during the crystallization process. This suggests that more diverse materials may be involved in the Hannuoba basalt magmatic system.

Plagioclase is an ideal material for strontium isotope analysis because of its high strontium content and low rubidium content, and it is a widely existing rock-forming mineral in igneous rocks. In the past few decades, with the development of analytical techniques, a large number of studies have begun to use in-situ Sr isotopes of plagioclase to reveal the complex evolutionary history of the magmatic system (Davidson et al., 2001; Davidson and Tepley, 1997; Ramos et al., 2004; Ramos et al., 2005; Tepley et al., 2000; Yan et al., 2020). Many researchers have found that the strontium isotope heterogeneity of plagioclase is far more significant than that of whole-rock scale (Edwards et al., 2019; Lange et al., 2013), and there is a significant strontium isotopic disequilibria between phenocrysts and matrix, as well as within a single grain, which is considered to be significant evidence of magma mixing, contamination and contribution of multiple source materials (Davidson et al., 2001). When the isotopic, minor, and trace elements data from the core to the rim of plagioclase are combined with the geochemical characteristics of the whole rock, the magma evolution history from crystal nucleation to eruption can be understood, and the crustal contamination and mixing of different mantle-derived magmas can be effectively distinguished, although some of the information might be lost due to the dissolution of plagioclase (Ginibre and Davidson, 2014; Hagen-Peter et al., 2019; Ramos and Reid, 2005).

Always consult and cite the final, published document. See http:/www.minsocam.org or GeoscienceWorld

This is the peer-reviewed, final accepted version for American Mineralogist, published by the Mineralogical Society of America.
The published version is subject to change. Cite as Authors (Year) Title. American Mineralogist, in press.
DOI: https://doi.org/10.2138/am-2022-8254. http://www.minsocam.org/

In this study, the in-situ strontium isotope, major and trace elements of plagioclase, combined with the major and trace elements of the whole rock, are used to clarify or explain the contribution of the lower continental crust during the formation of Hannuoba tholeiite. We find that the range of strontium isotope recorded by plagioclase is much more extensive than that recorded by Hannuoba alkaline and tholeiitic whole-rock compositions, but it is consistent with the observed range Cenozoic basalts in the North China Craton. Although the mixing of the alkaline basalt and the lower crust can explain that the content of trace elements in the Hanuoba tholeiite is between the Hanuoba alkaline basalt and the lower crust, the low 87Sr/86Sr (<0.704) characteristics of plagioclase cannot come from alkaline basalt, because trace element in the plagioclase is not in equilibrium with alkaline basalt. Therefore, we believe that the compositional heterogeneity of Hannuoba tholeiitic basalt is caused by mixing heterogeneous lower crust rather than the mixing of different mantle-derived melts, which indicates the contribution of continental lower crust to continental basalt is more complicated than previously recognized.

Geological setting and samples

The North China Craton is one of the three largest cratons in China (Fig.1A), which has attracted international attention due to its relatively complete record of geological events from Archean to Cenozoic (Zhao et al., 2001). Cenozoic continental intraplate basalts with geochemical characteristics of oceanic island basalts are widely distributed in the North China Craton (Chu et al., 2017; Fan and Hooper, 1991; Yang

Always consult and cite the final, published document. See http:/www.minsocam.org or GeoscienceWorld

This is the peer-reviewed, final accepted version for American Mineralogist, published by the Mineralogical Society of America.
The published version is subject to change. Cite as Authors (Year) Title. American Mineralogist, in press.
DOI: https://doi.org/10.2138/am-2022-8254. http://www.minsocam.org/

and Zhou, 2013; Zou, 2000). The Hannuoba basaltic area, located 200 Km northwest of Beijing (Fig.1A), is an important occurrence because of its large area (> 1700 Km^2), compositional diversity in intercalated tholeiitic and alkaline lavas, and abundant mantle xenoliths in the alkaline basalts (Zhi et al., 1990). Previous studies suggest that Hannuoba volcanism was controlled by deep fractures and ranges in age from Miocene in the east to Pliocene in the west (Fig.1B) (Zhi et al., 1990). Geochemical analysis of whole-rock and olivine hosted melt inclusions has indicated that Hannuoba tholeiitic basalts have relatively homogeneous characteristics of major and trace elements but vary significantly in radiogenic isotopes compared with the alkaline basalt (Jiang and Zhi, 2010; Qian et al., 2015; Song et al., 1990). Source heterogeneity, magma mixing, high-pressure fractionation, and crustal contamination have been suggested to account for compositional diversity in Hannuoba basalts (Jiang and Zhi, 2010; Qian et al., 2015; Song et al., 1990; Yang et al., 2016; Zhi et al., 1990). Three tholeiitic basalts samples studied in this paper were collected from the eastern part because they are well exposed, and the stratigraphy is clear (Fig.1B). Their spatial relationship is shown in Fig. 1C. Samples SQB03 and JSB04 are collected from the lavas erupted before the eruption of alkaline basalt, and JSB12 is collected from relatively late lavas after the eruption of alkaline basalt. (Fig. 1C).

Always consult and cite the final, published document. See http:/www.minsocam.org or GeoscienceWorld

This is the peer-reviewed, final accepted version for American Mineralogist, published by the Mineralogical Society of America.
The published version is subject to change. Cite as Authors (Year) Title. American Mineralogist, in press.
DOI: https://doi.org/10.2138/am-2022-8254. http://www.minsocam.org/

Analytical methods

Petrography and mineral major element analysis

Thin sections (30 μm thickness) were prepared from representative billets cut from the three samples, and optical and electrical microscopy was carried out on all thin sections to document petrographical features. High-resolution backscattered electron images were obtained at the Research Center of Genetic Mineralogy, China University of Geosciences (Beijing), using a field emission MIRA3 XMU scanning electron microscope. Electron-probe micro-analysis (EPMA) of individual plagioclase and clinopyroxene phenocrysts was carried out at Wuhan Sample Solution Analytical Technology Co., Ltd. using a JXA-8230 electron probe micro-analyzer (EPMA) under operating conditions of 20 nA, an accelerating voltage of 15 keV, and beam size of 1 μm in diameter for clinopyroxene and 3 μm for plagioclase. Peak and background counting times were 10 and 5 s for Si, Ca, Na, Al, Fe, and Mg, 20 and 10 s for Ti, Mn, Cr, K, Ni, and P. Analytical results were corrected using the ZAF correction routines. The standards used were SPI standard mineral and were analyzed as internal standards to monitor data quality. Analyses are accurate to 1–2% for major elements (>10 wt%) and 2–10% relative for minor elements (0.5–10% wt%). (Supplementary Tables 1,2 and 3)

In-situ mineral trace element analysis

In situ trace element analyses of plagioclase and clinopyroxene were carried out using laser ablation inductively coupled plasma mass spectrometry (LA-ICP-MS) in the mineral laser microprobe analysis laboratory (Milma laboratory) of China

Always consult and cite the final, published document. See http:/www.minsocam.org or GeoscienceWorld

This is the peer-reviewed, final accepted version for American Mineralogist, published by the Mineralogical Society of America.
The published version is subject to change. Cite as Authors (Year) Title. American Mineralogist, in press.
DOI: https://doi.org/10.2138/am-2022-8254. http://www.minsocam.org/

University of Geosciences (Beijing). The Agilent 7900 ICP-MS instrument was coupled to a resonetic 193 nm excimer laser ablation system. Single spot ablation was adopted with a laser beam of 50 μm, and ablation frequency was 8 Hz. Helium gas was used as a carrier gas. The detailed parameter settings of the instrument and experimental process can be found in (Zhang et al., 2019). NIST610 was used as an external standard, while ^{43}Ca was selected as the internal standard to correct the element composition. The Ca content in the samples is from the data obtained by EPMA. The precise value of Ca content in NIST 610 can be seen in (Jochum et al., 2011). The trace elements data were processed using the Iolite software based on the Igor platform (Paton et al., 2011). We analyzed the USGS reference glass BCR-2G as an unknown sample, and the results were within the error range of the recommended values (Supplementary Tables 4 and 5) which may be referred to (Jochum et al., 2005). The analytical uncertainty is better than 10% (relative).

In-situ Sr isotope analysis

In-situ Sr isotope measurements were performed on a Neptune Plus MC-ICP-MS (Thermo Fisher Scientific, Germany) in combination with a J-200 343 nm femtosecond laser ablation system (Applied Spectra, USA) housed at the National Research Center for Geoanalysis, Chinese Academy of Geological Sciences (CAGS), Beijing, China. The JET sample and X skimmer cones were used along with the guard electrode (GE), and all measurements were conducted under the low resolution and static mode. At the beginning of every analytical session, the fs-LA-ICP-MS system was optimized using NIST 612 to achieve maximum signal intensity and low oxide

Always consult and cite the final, published document. See http:/www.minsocam.org or GeoscienceWorld

This is the peer-reviewed, final accepted version for American Mineralogist, published by the Mineralogical Society of America.
The published version is subject to change. Cite as Authors (Year) Title. American Mineralogist, in press.
DOI: https://doi.org/10.2138/am-2022-8254. http://www.minsocam.org/

198 rates. Samples were ablated inline mode with a spot size of 30 μm, line length of 20
199 μm, stage movement speed of 0.65 μm/s, laser repetition rate of 8 Hz, and beam
200 energy density of 1.5 J/cm^2. The instrumental mass bias for Sr isotopes was corrected
201 using an exponential law function based on $^{86}Sr/^{88}Sr$ value of 0.1194. Correction of
202 interferences of Kr isotopes on mass 84 and 86 was accomplished by background
203 subtraction. The interferences of doubly charged ions of $^{168}Er^{2+}$ on ^{84}Sr, $^{170}Er^{2+}$ and
204 $^{170}Yb^{2+}$ on ^{85}Rb, $^{172}Yb^{2+}$ on ^{86}Sr, and $^{174}Yb^{2+}$ on ^{87}Sr were corrected based on the
205 measured signal intensities of $^{167}Er^{2+}$ (m/z 83.5) and $^{173}Yb^{2+}$ (m/z 86.5) and the natural
206 isotopic composition of Rb, Er and Yb (Li et al., 2018). The determined $^{87}Sr/^{86}Sr$ of
207 Durango standard was 0.70675 ± 0.00012 (2SD, n = 9) (Supplementary Table 6),
208 which is slightly higher than the results determined by previous studies with $^{87}Sr/^{86}Sr$
209 of 0.70629 ± 00002 to 0.70638 ± 0.00013 (2SD, n = 8) (Yang et al., 2014) and
210 references therein; however, $^{87}Sr/^{86}Sr$ for every single point ranges from 0.70670 ±
211 0.00027 to 0.70689 ± 0.00033 (2SE) which is consistent with the literature results
212 within the error range. $^{84}Sr/^{86}Sr$ was also monitored during analyses, and the average
213 values are 0.05596 ± 0.00034 (2SD, n = 9) for Durango standard and 0.05667 ±
214 0.0028 for all in-situ plagioclase points, which agree well with the "true" value of
215 0.0565 (2SD, n = 27). Further analysis of the reliability of the Sr isotope data will be
216 presented in the discussion section.

217 **Whole-rock major and trace element analysis**

218 Quantitative analyses of major elements contents in whole rocks were conducted
219 using X-ray Fluorescence Spectrometer (XRF) at the Ore Deposit Geochemistry

Always consult and cite the final, published document. See http:/www.minsocam.org or GeoscienceWorld

This is the peer-reviewed, final accepted version for American Mineralogist, published by the Mineralogical Society of America.
The published version is subject to change. Cite as Authors (Year) Title. American Mineralogist, in press.
DOI: https://doi.org/10.2138/am-2022-8254. http://www.minsocam.org/

Microanalysis Laboratory, affiliated to the State Key Laboratory of Geological Processes and Mineral Resources, China University of Geosciences (Beijing). The laboratory is equipped with Shimadzu's wavelength dispersive X-ray fluorescence spectrometer. The fused beads method was used in the preparation of test specimens. Mixed weighed amounts of sample and flux and placed the mixture in a clean platinum/gold crucible. A 0.7 g of sample (200 mesh) plus 7.0 g of mixed lithium borate fluxes were used in this study. The addition of a small amount (100 mg) of a halide, such as LiBr, acted as a release agent when using platinum/gold molds. The mixture was heated in a high-frequency fusion machine at a fixed temperature, usually from 950 °C to 1100 °C, until thoroughly melted. Then the fused beads were loaded into the XRF instrument for determination; the fusion time was about 30 min. The measurement procedure and data quality were monitored by repeat analysis of international basalt standards BCR-2 and BHVO-2. The analytical precision (RSD, relative standard deviation) and accuracy (RE, relative error between measured and recommended values) are better than 5% for major elements, with many elements agreeing to within 2% of the reference values (Supplementary Table 7).

All whole-rock trace element compositions were measured by ICP-MS (Agilent 7500a with a shielded torch) at the State Key Laboratory of Geological Processes and Mineral Resources, China University of Geosciences (Wuhan). The detailed sample-digestion procedure for ICP-MS analyses has been described by (Liu et al., 2008a). The reproducibility is better than 5% (RSD) for all elements. The accuracy, determined relative to reference values of BHVO-2 and BCR-2, is better than 5% (RE)

Always consult and cite the final, published document. See http:/www.minsocam.org or GeoscienceWorld

This is the peer-reviewed, final accepted version for American Mineralogist, published by the Mineralogical Society of America.
The published version is subject to change. Cite as Authors (Year) Title. American Mineralogist, in press.
DOI: https://doi.org/10.2138/am-2022-8254. http://www.minsocam.org/

(Supplementary Table 7).

Results

Petrography

Representative thin-section photographs of the samples are presented in Figure 2. The petrographic characteristics of the basalts may be divided into a fine-grained group (samples SQB03A, SQB03B, and JSB04) and a coarse-grained group (sample JSB12). For the fine-grained group, the most common phenocryst phase is plagioclase feldspar (~10-15 vol%), followed by clinopyroxene (~5-10 vol%) with trace amounts of olivine (<5 vol%). The plagioclase phenocrysts are euhedral and tabular, with sizes (length) ranging from ~400 μm to ~3 mm, and crystals of all sizes exhibit concentric zoning. Clinopyroxene phenocrysts are euhedral to rounded and commonly form glomerocrysts with plagioclase and olivine (Figure 2). Simple twinning of clinopyroxene is common, and phenocrysts range up to ~1 mm in size. Equant olivine phenocrysts (0.2–2 mm) are present. All phenocrysts are set in fine-grained plagioclase, clinopyroxene, olivine, and Fe-Ti oxide matrix. Although the overall grain size of the coarse-grained group is larger than that of the fine-grained group, its phenocrysts and matrix minerals are not easy to distinguish (sample JSB12 in Fig. 2). For the coarse-grained group, the major rock-forming minerals are plagioclase (~45 vol%) and clinopyroxene (~25 vol%), followed by olivine(~15 vol%) and K-feldspar (~10 vol%) with small amounts of Fe-Ti oxide (~5 vol%). Plagioclase phenocrysts are typically tabular-shaped in all the samples. The most significant difference between

Always consult and cite the final, published document. See http:/www.minsocam.org or GeoscienceWorld

This is the peer-reviewed, final accepted version for American Mineralogist, published by the Mineralogical Society of America.
The published version is subject to change. Cite as Authors (Year) Title. American Mineralogist, in press.
DOI: https://doi.org/10.2138/am-2022-8254. http://www.minsocam.org/

the fine-grained and coarse-grained samples is that the former has an overall smaller grain size but has some larger plagioclase phenocrysts (Fig. 2).

Whole-rock major and trace element

Whole-rock major and trace element data are presented in Supplementary Table 7. All the samples are classified as basalt (Supplementary Fig. 1) and plot within the range of Hannuoba tholeiitic basalt samples collected previously (Zhi et al., 1990). The visible freshness of the lavas chosen for this study is confirmed by low loss on ignition (LOI) values that range from 0.15 to 3.01 wt%, and the minerals in the samples are fresh and have not undergone alteration. Compared with the fine-grained samples, the coarse-grained samples have higher TiO_2, FeO, K_2O, and P_2O_5 content. Other oxides contents are very similar in the two types of samples.

All the samples have a smooth chondrite-normalized rare earth element (REE) pattern with a slight positive Eu anomaly (Supplementary Fig. 2,3). LREE and MREE contents in the coarse-grained samples are higher than those in the fine-grained samples, but their HREE contents are similar. Abundances of trace elements, normalized to values for the primitive mantle (McDonough and Sun, 1995), show typical continental oceanic island basalt-like pattern with marked depletion in Pb, Th, and U, and enrichments in Ba, Nb, Ta, and Sr (Fig. 3), which is consistent with data reported previously (Qian et al., 2015; Zhi et al., 1990). All the incompatible element contents and Ce/Pb, Nb/U, and Nb/La ratios in the coarse-grained samples are higher than those in the fine-grained samples (Supplementary Table 7).

Always consult and cite the final, published document. See http:/www.minsocam.org or GeoscienceWorld

This is the peer-reviewed, final accepted version for American Mineralogist, published by the Mineralogical Society of America.
The published version is subject to change. Cite as Authors (Year) Title. American Mineralogist, in press.
DOI: https://doi.org/10.2138/am-2022-8254. http://www.minsocam.org/

Mineral major and trace element

The major and trace element data of all minerals are provided in Supplementary Tables 1-5. From the backscattered electron (BSE) images, it can be observed from Fig.4 that compositional zoning in plagioclase within a given sample generally consists of only oscillatory zoning type, and zoning is consistent between crystals. Representative backscattered electron images of four individual plagioclase crystals from the three samples and variation trends diagrams for An, Mg, Ti, and Sr from the interior to the rim are shown in Fig. 4. Given that the spot size for in-situ trace element measurement is ~50μm, which is significantly wider than the width for a single zoning, detailed EPMA data with data point distance ranging from 5μm to 40μm are shown in Fig. 5 and Supplementary Table 2.

Plagioclase phenocrysts in the fine-grained samples (SQB03A, SQB03B, and JSB04) are oscillatory zoned, with occasional dissolution surfaces. The An content fluctuates between 57 and 64 when the distance from the rim is more than 100μm (Figs 4 and 5) and decreases significantly to 32~56 in the rim as displayed by EMPA profiles (Fig. 5). Mg and Sr are positively correlated with An content, while other trace elements are scattered at a given An content (Fig. 6). Partially resorbed zones are richer in Ca (An=62~64)，Sr (800~900 ppm) and Mg (>1000 ppm) than other zones (Fig. 4), which is interpreted as reflecting a more mafic recharge event by a Ca and Sr richer magma.

Plagioclase phenocrysts in the coarse-grained sample JSB12 are also oscillatory zoned but generally more sodic than those in the fine-grained samples. Two different

Always consult and cite the final, published document. See http:/www.minsocam.org or GeoscienceWorld

This is the peer-reviewed, final accepted version for American Mineralogist, published by the Mineralogical Society of America.
The published version is subject to change. Cite as Authors (Year) Title. American Mineralogist, in press.
DOI: https://doi.org/10.2138/am-2022-8254. http://www.minsocam.org/

oscillatory zones may be identified, inner calcic zones with An fluctuate between 54 and 62 and outer sodic zones with An fluctuate between 48 and 57 (Fig. 5). The zone with dissolution surface mainly occurs in the inner zones and has a thickness ranging from 5 to 20μm. Partially resorbed zones with the embayed surface are richer in Ca (An=60~62) and Sr (1150~1300ppm) than other zones (Fig. 4). Sr is positively correlated with An content, while other trace elements are scattered at a given An content, and Ti, Sr, Ba, La, and Eu contents are generally higher than those in the fine-grained samples (Fig. 6).

The chondrite-normalized diagram (supplementary Fig. 3) drawn according to the in-situ trace element data of plagioclase indicates that plagioclase phenocrysts from all the studied samples show enrichment in light rare earth elements and strong Eu positive anomalies. Variation of Eu anomalies ranges from 1.52 to 9.94. Except for a few individual data, the abundance of rare earth elements in plagioclase phenocrysts from the coarse-grained sample (JSB12) is higher than that in the other three fine-grained samples. The clinopyroxene phenocrysts in the two groups have comparable major element characteristics and range from En_{43} Fs_{12} Wo_{44} to En_{46} Fs_{12} Wo_{41} (Supplementary Table 3). All the clinopyroxene REE data show a similar pattern with enriched MREE compared with LREE and HREE (Figure 7), and the coarse-grained sample has overall higher LREE and lower HREE concentrations than those in the fine-grained samples.

Always consult and cite the final, published document. See http:/www.minsocam.org or GeoscienceWorld

This is the peer-reviewed, final accepted version for American Mineralogist, published by the Mineralogical Society of America.
The published version is subject to change. Cite as Authors (Year) Title. American Mineralogist, in press.
DOI: https://doi.org/10.2138/am-2022-8254. http://www.minsocam.org/

Sr isotope in plagioclase

The $^{87}Sr/^{86}$ Sr ratios of plagioclase phenocrysts are presented in Supplementary Table 6. All four plagioclase phenocrysts show large variation (>0.001) in $^{87}Sr/^{86}$ Sr ratio, with the lowest ratio_of 0.70333 ± 0.00018 (2SE) in sample JSB12 and the highest ratio of 0.70556 ± 0.00031 (2SE) in sample SQB03A (Figure 8). The average $^{87}Sr/^{86}Sr$ of the fine-grained samples are 0.70434 ± 0.00112 (2SD) (SQB03A), 0.70471 ± 0.00102 (2SD) (SQB03B) and 0.70455 ± 0.00074 (2SD) (JSB04), which all higher than the coarse-grained sample JSB12-1 of 0.70425 ± 0.00109 (2SD). The variation of strontium isotope recorded by plagioclase is much larger than that recorded by Hannuoba alkaline and tholeiitic whole rocks (Song et al., 1990), but it is consistent with the variation range of Cenozoic basalts in North China Craton (Fig. 9). Partially resorbed zones with higher An contents may have either higher or lower $^{87}Sr/^{86}$ Sr ratios than other zones in the fine-grained samples, the variation of Sr isotope value may be characteristic of the dissolution zone or may be caused by the adjacent bands (Fig. 9). Sample SQB03A show similar correlation trends between An and $^{87}Sr/^{86}$ Sr ratios with sample SQB03B, except the two rim points (Fig. 9), suggesting a similar crystallization process occurred for different individual crystals, which is consistent with their comparable zoning pattern as displayed by BSE images (Figure 8). For sample JSB04, rim and core have a higher $^{87}Sr/^{86}$ Sr ratio than other zones. In contrast, partially resorbed zones in sample JSB12 are accompanied by a significant decrease in the $^{87}Sr/^{86}$ Sr ratio and an abrupt increase in the rim zones.

Always consult and cite the final, published document. See http:/www.minsocam.org or GeoscienceWorld

This is the peer-reviewed, final accepted version for American Mineralogist, published by the Mineralogical Society of America.
The published version is subject to change. Cite as Authors (Year) Title. American Mineralogist, in press.
DOI: https://doi.org/10.2138/am-2022-8254. http://www.minsocam.org/

348 **Thermobarometers**

349 The REE in plagioclase-clinopyroxene geothermometer (Sun and Liang, 2017)
350 gives crystallization temperatures of 1088~1156℃ for the fine-grained samples and
351 1113~1129℃ for the coarse-grained sample (Supplementary Table 8.). Temperatures
352 calculated from the Mg-Ca coupled exchange thermometer of plagioclase and
353 clinopyroxene (Sun and Lissenberg, 2018) are 1078~1134℃ for the fine-grained
354 samples and 1076~1079℃ for the coarse-grained samples (Supplementary Table 8.).
355 Given that the two different thermometers were applied to the same samples, the
356 systematic differences between T_{Mg} and T_{REE} (Figure 10) are most likely due to the
357 differential diffusive responses of Mg and REE to changes in temperature after
358 crystallization of the cumulus minerals. The average difference between T_{Mg} and T_{REE}
359 (Figure 10) indicates that crystallization occurs within the range of 20℃ (fine-grained
360 basalt) and 50℃(coarse-grained basalt).The crystallization of these samples are
361 complete within 20 to 50℃ before eruption, which may be a reason for the textural
362 differences between the two types of basalts. The inverted initial temperatures
363 (1120-1140 °C) by Mg-REE coupled geothermometer are very close to T_{REE}
364 (1088-1156 °C), indicating a small diffusive redistribution of REE in Hannuoba basalt.
365 Cooling rates calculated by Mg-REE coupled geospeedometer (Sun and Lissenberg,
366 2018) suggest that the coarse-grained sample generally (0.004 °C/yr) cooled slower
367 than the fine-grained samples (0.0004–0.05 °C/yr), although a small number of
368 results, possibly due to the large error, are abnormal. (Supplementary Table 8.).

369 Clinopyroxene-melt equilibrium thermometer Eq.33 of (Putirka, 2008) and

Always consult and cite the final, published document. See http:/www.minsocam.org or GeoscienceWorld

This is the peer-reviewed, final accepted version for American Mineralogist, published by the Mineralogical Society of America.
The published version is subject to change. Cite as Authors (Year) Title. American Mineralogist, in press.
DOI: https://doi.org/10.2138/am-2022-8254. http://www.minsocam.org/

barometer of (Neave and Putirka, 2017) have been suggested as the most accurate and precise thermobarometer. Crystallization temperatures and pressures calculated from the thermobarometer are 1129~1189 ℃ and 0.7 ~4.4 Kbar for the fine-grained samples, and 1149~1159℃ and 3.9 ~4.3 Kbar for the coarse-grained samples. The temperatures are slightly higher than T_{REE} but agree within error (Supplementary Table 8.). The temperature obtained by the rare earth element thermometers may be regarded as the crystallization temperature of the phenocrysts because 1) the error on the rare earth element exchange thermometers of plagioclase and pyroxene is smaller than that of the pyroxene thermometers and 2) the rare earth element thermometers are less affected by pressure and water concentrations (Sun and Liang, 2017).

Because the plagioclase mineral-melt equilibrium thermobarometer is significantly affected by the water content in the melt (Putirka, 2008) and the initial water content in Hannuoba tholeiitic basalt is unknown, this thermobarometer was not considered in this study.

Discussion

Reliability of in situ Sr isotope data

Possible interference with in situ Sr isotope analysis includes Kr and Rb and other elements (see Analytical methods section and Li et al. (2018)). Trace amounts of Kr may exist as impurities in trace amounts of argon, which may affect the accuracy of the data, because ^{84}Kr and ^{86} Kr interfere with ^{84}Sr and ^{86}Sr signals, respectively. This interference was corrected by measuring the Kr blank of the gas, and based on the

Always consult and cite the final, published document. See http:/www.minsocam.org or GeoscienceWorld

This is the peer-reviewed, final accepted version for American Mineralogist, published by the Mineralogical Society of America.
The published version is subject to change. Cite as Authors (Year) Title. American Mineralogist, in press.
DOI: https://doi.org/10.2138/am-2022-8254. http://www.minsocam.org/

measured $^{87}Sr/^{86}Sr$ ratio at the known apatite standard, the effect proved to be valid. ^{87}Rb is a significant interference for Sr isotopic analysis. Generally, an analysis of ^{85}Rb is needed for corrections. The content of Rb in the plagioclase samples from Hannuoba basalts is relatively low (<1ppm), which indicates that ^{87}Rb has a minimal interference to the Sr isotope (<0.00001).

All the LA-ICPMS Sr isotope data in this study have more significant analytical error (0.00024 of average 2σ error) than micro-drilling data (Davidson et al., 2001; Ginibre and Davidson, 2014) mainly due to the spot size of 30μm. The accuracy of the data may be ensured because the data for the Durango standard analyzed in this study agree well with the recommended values and within the analytical error. On the other hand, the Sr isotope data for the compositional zones of plagioclase with a thickness less than 50μm are very close or nearly indistinguishable (Figure 9), suggesting that the precision of the Sr isotope is high enough to capture the isotopic heterogeneities within individual plagioclase crystal.

Magma mixing recorded in compositional and isotopic zoning

There are at least three mechanisms to explain the variation in the An content of the plagioclase: a hotter magma underplating increased the temperature of the magma, leading to an increase in An content of plagioclase; reductions in the water content of the melt through degassing or removing volatile fluids; changes in the composition of the melt caused by magma recharge. We may distinguish these processes using abundances and patterns of slow diffusing trace elements in plagioclase phenocrysts because each process should result in different trace element responses and patterns.

Always consult and cite the final, published document. See http:/www.minsocam.org or GeoscienceWorld

This is the peer-reviewed, final accepted version for American Mineralogist, published by the Mineralogical Society of America.
The published version is subject to change. Cite as Authors (Year) Title. American Mineralogist, in press.
DOI: https://doi.org/10.2138/am-2022-8254. http://www.minsocam.org/

414 The An values of Hannuoba samples varied between 56 and 64. We assume that
415 the melt's composition (not including volatiles) remains the same, and the changes of
416 the An values may be caused by a modest increase in temperature or by the reduction
417 of H_2O content in the melt. Although temperature does affect the distribution of Sr
418 between plagioclase and siliceous melt, this effect does not affect the relationship
419 between An value and Sr (Bindeman et al., 1998). Using the partition coefficient of
420 Bindeman et al. (1998), to change the temperature by 100°C as suggested by the
421 plagioclase REE thermometer would only change the concentration of Sr in
422 plagioclase 10-15ppm. Moreover, at a given temperature, when the An content varies
423 from 56 to 64, the Sr partition coefficient could only change 20%. However, the Sr
424 variation in the plagioclase phenocrysts in Hannuoba basalts is far beyond this range
425 (Figure 6). Therefore, changes in the concentration of trace elements and An in
426 plagioclase are not caused by changes in temperature alone. Blundy and Wood (1991)
427 found that there is almost no difference in the distribution coefficient of Sr between
428 hydrothermal and silicate melts, which means that H_2O has only a weak effect on the
429 distribution coefficient of Sr. Therefore, zoning patterns in plagioclase is most likely
430 attributable to changes in melt composition, and changes in melt chemistry that may
431 accompany changes in melt temperature and H_2O content.

432 The dissolution surface and the oscillatory changes in An content（Fig. 5）suggest
433 compositionally distinct pulses of melt. Also, the intracrystalline Sr isotope data suggest
434 some episodes of magma recharge are occurring.

435 Thus, magma mixing could be responsible for the compositional and isotopic

Always consult and cite the final, published document. See http:/www.minsocam.org or GeoscienceWorld

This is the peer-reviewed, final accepted version for American Mineralogist, published by the Mineralogical Society of America.
The published version is subject to change. Cite as Authors (Year) Title. American Mineralogist, in press.
DOI: https://doi.org/10.2138/am-2022-8254. http://www.minsocam.org/

diversity in the plagioclase phenocrysts. The relatively large size of the LC-ICPMS laser spot compared to the width of the individual oscillatory zones results in the simultaneous analysis of multiple zones, providing an averaged composition, so the observed variation should be considered a minimum. Even with the limited spatial resolution of the laser-ablation system, our data demonstrate that some plagioclase phenocrysts in Hannuoba basalts preserve significant isotopic variation and that the Sr isotope compositions of these crystals are commonly higher or lower than bulk-rock $^{87}Sr/^{86}Sr$ in Hannuoba basalts (Figure 9). To preserve intracrystalline Sr isotopic disequilibria on the scale of 30 μm or less, plagioclase phenocrysts cannot have been kept at magmatic temperatures (~1000°C) for significant periods (100 years) because this would result in diffusive re-equilibration (Davidson et al., 2001; Ramos and Reid, 2005). This is consistent with the fast cooling rate obtained from plagioclase-clinopyroxene Mg-REE coupled geospeedometer (Sun and Lissenberg, 2018) and a small diffusive redistribution of REE in Hannuoba basalt. The intracrystalline disequilibria were most likely generated during episodic crystal growth through interaction with isotopically distinct melts at crustal pressures, possibly within the middle-crust magma chamber or plumbing system as recorded by crystallization pressures from the barometer of clinopyroxene.

Contamination of heterogeneous continental lower crust

Two hypotheses have been proposed to account for compositional and isotope variations in Hannuoba basalts. The first attributes them to the mixing of basaltic melts generated from compositionally and isotopically distinct mantle sources with

Always consult and cite the final, published document. See http:/www.minsocam.org or GeoscienceWorld

This is the peer-reviewed, final accepted version for American Mineralogist, published by the Mineralogical Society of America.
The published version is subject to change. Cite as Authors (Year) Title. American Mineralogist, in press.
DOI: https://doi.org/10.2138/am-2022-8254. http://www.minsocam.org/

458 negligible crustal contamination based on trace elements and Sr-Nd-Pb isotopic
459 characteristics (Qian et al., 2015; Song et al., 1990; Zhi et al., 1990). The second
460 suggests that the compositional characteristics result from mantle melts assimilating
461 crustal components (Jiang and Zhi, 2010) based on very high $^{187}Os/^{188}Os$. Although
462 the Nb/U ratio in Hannuoba alkaline and tholeiitic basalts are significantly higher than
463 average continental crust (Qian et al., 2015), lower crust contamination cannot be
464 excluded because the Nb/U ratio in the lower continental crust has been suggested to
465 be very heterogeneous (Gao et al., 1998; Huang et al., 2004; Rudnick and Fountain,
466 1995), and mafic lower crustal materials can have Nb/U up to 50 (Rudnick and
467 Fountain, 1995), which is very close to the values documented in the Hannuoba
468 tholeiitic basalts (Nb/U=46~51). In addition, the $^{187}Os/^{188}Os$ of the Hannuoba
469 tholeiites (0.15882 - 0.61607) are mostly higher than those of the transitional basalts
470 (0.23425-0.35779) and alkaline basalts (0.14869- 0.29528) (Jiang and Zhi, 2010), and
471 they are significantly higher than those of the lithospheric mantle, suggesting that
472 crustal contamination is widespread in the Hannuoba basalts. Therefore, the best
473 explanation for the EMI characteristics of the enriched radiogenic strontium isotopes
474 of the Hannuoba tholeiites seems to be contamination by the lower continental crust.

475 The significant change of $^{87}Sr/^{86}Sr$ ratio is likely due to assimilation of Hannuoba
476 alkaline basalts by lower continental crust because the former has significantly lower
477 $^{87}Sr/^{86}Sr$. However, trace element contents in the melt that are in equilibrium with the
478 plagioclase, calculated using the Bindeman et al. (1998) model, show minimal
479 variation (Figure 11, Supplementary Table 9), and Sr and Ba contents similar to that in

Always consult and cite the final, published document. See http:/www.minsocam.org or GeoscienceWorld

This is the peer-reviewed, final accepted version for American Mineralogist, published by the Mineralogical Society of America.
The published version is subject to change. Cite as Authors (Year) Title. American Mineralogist, in press.
DOI: https://doi.org/10.2138/am-2022-8254. http://www.minsocam.org/

tholeiitic basalts, but significantly lower than those in alkaline basalts, suggesting that, at least, Hannuoba alkaline basaltic melts were not directly contributing to the intracrystalline Sr isotopic disequilibria. Other trace elements such as La and Eu are either lower or higher than that in tholeiitic basalts (Figure 11), which is possibly due to model uncertainty as shown by many other experimental and theoretical studies (Bedard, 2006; Bindeman et al., 1998). Given that trace element content in Hannuoba tholeiite is between Hannuoba alkaline basalts and lower continental crust (Figure 3), mixing of Hannuoba alkaline basalts and the lower continental crust can explain the bulk rock compositional characteristic of Hannuoba tholeiite, which is also consistent with intercalated tholeiitic and alkaline lavas. However, in this case, the low $^{87}Sr/^{86}Sr$ (<0.704) signature in plagioclase cannot be from alkaline basaltic melts. It is likely that the alkali basalt interacted with the lower continental crust and formed a mixed magma. The trace element abundances and ratios in this magma are similar to the Hannuoba tholeiite and relatively homogeneous, but the isotopes are heterogeneous. The crystalline plagioclase will inherit the decoupled isotopic and trace element characteristics when the magma rises and injects into the magma chamber. The Hannuoba tholeiite crystallized within a 20 ℃ (fine-grained basalt) and 50℃ (coarse-grained basalt) temperature window also suggest that compositionally (major and trace element) similar magmas were mixed with each other before the eruption. This understanding is similar to that obtained from the study of melt inclusions: the Pb isotope variation range of melt inclusions entrapped in olivine in a Hannuoba tholeiite vary significantly and extend toward an EM1-type isotopic

Always consult and cite the final, published document. See http:/www.minsocam.org or GeoscienceWorld

This is the peer-reviewed, final accepted version for American Mineralogist, published by the Mineralogical Society of America.
The published version is subject to change. Cite as Authors (Year) Title. American Mineralogist, in press.
DOI: https://doi.org/10.2138/am-2022-8254. http://www.minsocam.org/

composition, similar to that of all tholeiites, but the variation range of major and minor elements is relatively tiny (Qian et al., 2015).

The potential problem is that the major and trace elements and isotopes in the lower crust are quite heterogeneous. If significant isotope heterogeneity is recorded in plagioclases in the two types of tholeiitic basalts in Hannuoba, then it would be expected that the strontium isotope ratios would be lower than those for the average lower continental crust. This may be related to the highly compositional heterogeneity and multi-stage evolution of the lower crust in the North China Craton (Jiang et al., 2013; Liu et al., 2004). Previous studies have shown that strontium isotopes in the lower crust of the North China Craton vary from 0.704 to 0.746, and strontium contents vary from < 100ppm to > 1500ppm (Jiang et al., 2013; Liu et al., 2004). The major and trace elements in the lower crust (probably local) may be relatively homogeneous due to the long-term and multi-stage magmatic underplating, but the isotopic heterogeneity is still significant. In addition, it should be noted that the contents of trace elements in the whole rock and plagioclase of the two types of Hannuoba basalts are different, which indicates that there are differences in the parent magma itself. This difference may be caused by the heterogeneity of local lower crust materials, or it may be the product of magma evolution by crystallization and differentiation after mixing alkaline basaltic rocks and different proportions of the lower crust. Our current research does not distinguish between these possibilities. In general, the contribution of lower crustal contamination to the formation of Hannuoba tholeiite is more complex than previously thought. Identifying the existence of lower

Always consult and cite the final, published document. See http:/www.minsocam.org or GeoscienceWorld

This is the peer-reviewed, final accepted version for American Mineralogist, published by the Mineralogical Society of America.
The published version is subject to change. Cite as Authors (Year) Title. American Mineralogist, in press.
DOI: https://doi.org/10.2138/am-2022-8254. http://www.minsocam.org/

crust contamination on the basis of whole-rock geochemical characteristics and the average composition of the lower crust is challenging. However, in-situ trace elements and isotopes of plagioclase may help solve these problems.

Implication

Although the plagioclase phenocryst zoning in Hannuoba tholeiite is oscillatory and normal, and the content of anorthite and trace elements in each plagioclase grain does not vary significantly, which is similar to the oscillatory zoning formed by a closed system, the strontium isotope in the plagioclase micro area shows significant isotope disequilibrium. Moreover, the range of strontium isotope ratios is far more than that of all Hannuoba basalts, which has not been found in previous studies. Although the error on strontium isotope ratios is significant, we have detected greater than expected isotopic variation. If the beam spot increases, the error will decrease, but the observed isotope heterogeneity will be reduced or eliminated.

Because the isotopic heterogeneity of plagioclase zoning occurs in the crystallization process at the depths of the middle crust, both the lower crust and the upper mantle of the continent may contribute to the heterogeneity of magma, and the contamination and magma mixing may mainly occur in the lower crust and/or the upper mantle. Our study suggests that the contamination by the lower continental crust is more critical because the addition of material from the lower continental crust can explain the very high osmium isotope, the typical EMI type Sr-Nd-Pb isotope, and the lower incompatible element content of tholeiitic basalts compared with alkaline basalts. This phenomenon may be shared in Cenozoic basalts in eastern

Always consult and cite the final, published document. See http:/www.minsocam.org or GeoscienceWorld

This is the peer-reviewed, final accepted version for American Mineralogist, published by the Mineralogical Society of America.
The published version is subject to change. Cite as Authors (Year) Title. American Mineralogist, in press.
DOI: https://doi.org/10.2138/am-2022-8254. http://www.minsocam.org/

China; However, previous studies have attributed the compositional characteristics of EMI endmembers to the continental lithosphere, recycled continental or oceanic crust materials. An important reason for this phenomenon is that previous studies usually exclude contamination of the lower crust by comparing the whole rock composition characteristics with the global average continental lower crust composition, but this practice has a substantial uncertainty because the continental lower crust has significant compositional heterogeneity (Jiang et al., 2013; Liu et al., 2004; Rudnick and Fountain, 1995). The mafic lower crust may have a high degree of partial melting, mixing, and evolution, and then injected into the magma chamber of the shallow crust, resulting in heterogeneous geochemical characteristics and even leading to the decoupling of isotopes and trace elements, similar to those recorded in the plagioclase micro zonation in this study.

Another important finding of this study is that there are significant differences in petrography and trace element contents in mineral micro areas between the two types of tholeiites with different whole-rock compositions, which indicates that the magma with different initial compositions has undergone different crystallization history. The crystallization process of the two tholeiites might occur in an independent magma chamber or plumbing system. The in-situ study of mineral composition and isotope at the micro-regional scale, and the selection of basalts with significant differences in petrography, will help to reveal the complex evolutionary process of the magmatic system and is also of great significance for a comprehensive understanding of the origin and genesis of continental basaltic magma.

Always consult and cite the final, published document. See http:/www.minsocam.org or GeoscienceWorld

This is the peer-reviewed, final accepted version for American Mineralogist, published by the Mineralogical Society of America.
The published version is subject to change. Cite as Authors (Year) Title. American Mineralogist, in press.
DOI: https://doi.org/10.2138/am-2022-8254. http://www.minsocam.org/

568

569 **Acknowledgments**

570 Thanks to Zhang Liangliang and others from the Milia Laboratory of China
571 University of Geosciences (Beijing) for their help in the in-situ trace element
572 experiment, and Li Chao from the national testing and experimental center of the
573 Chinese Academy of Geological Sciences for help in the in situ strontium isotope
574 experiment. We thank an anonymous reviewer and Jenna Adams for their constructive
575 and thorough reviews. In addition, thanks to the comments and editorial work from
576 Professor Callum Hetherington. This work is supported by the Fundamental Research
577 Funds for the Central Universities (2652019049), the national college students'
578 innovation and entrepreneurship training program (202011415009), and the 111
579 project (B18048). This is CUGB petro-geochemical contribution No. PGC-2015##.

580 **References**

581 Basu, A.R., Wang, J.W., Huang, W.K., Xie, G.H., Tatsumoto, M., 1991. Major
582 Element, Ree, and Pb, Nd and Sr Isotopic Geochemistry of Cenozoic
583 Volcanic-Rocks of Eastern China - Implications for Their Origin from
584 Suboceanic-Type Mantle Reservoirs. Earth and Planetary Science Letters,
585 105(1-3): 149-169.

586 Bedard, J.H., 2006. Trace element partitioning in plagioclase feldspar. Geochimica Et
587 Cosmochimica Acta, 70(14): 3717-3742.

588 Bindeman, I.N., Davis, A.M., Drake, M.J., 1998. Ion microprobe study of
589 plagioclase-basalt partition experiments at natural concentration levels of trace

Always consult and cite the final, published document. See http:/www.minsocam.org or GeoscienceWorld

This is the peer-reviewed, final accepted version for American Mineralogist, published by the Mineralogical Society of America.
The published version is subject to change. Cite as Authors (Year) Title. American Mineralogist, in press.
DOI: https://doi.org/10.2138/am-2022-8254. http://www.minsocam.org/

elements. Geochimica Et Cosmochimica Acta, 62(7): 1175-1193.

Blundy, J.D., Wood, B.J., 1991. Crystal-Chemical Controls on the Partitioning of Sr and Ba between Plagioclase Feldspar, Silicate Melts, and Hydrothermal Solutions. Geochimica Et Cosmochimica Acta, 55(1): 193-209.

Chu, Z. et al., 2017. Petrogenesis of Cenozoic basalts in central-eastern China: Constraints from Re–Os and PGE geochemistry. Lithos, 278–281: 72-83.

Davidson, J., Tepley, F., Palacz, Z., Meffan-Main, S., 2001. Magma recharge, contamination and residence times revealed by in situ laser ablation isotopic analysis of feldspar in volcanic rocks. Earth and Planetary Science Letters, 184(2): 427-442.

Davidson, J.P., Tepley, F.J., 1997. Recharge in volcanic systems: Evidence from isotope profiles of phenocrysts. Science, 275(5301): 826-829.

Edwards, M.A. et al., 2019. Extreme enriched and heterogeneous 87Sr/86Sr ratios recorded in magmatic plagioclase from the Samoan hotspot. Earth and Planetary Science Letters, 511: 190-201.

Eisele, J., Sharma, M., Galer, S.J.G., Blichert-Toft, J., Devey, C.W., and Hofmann, A.W. (2002) The role of sediment recycling in EM-1 inferred from Os, Pb, Hf, Nd, Sr isotope and trace element systematics of the Pitcairn hotspot. Earth and Planetary Science Letters, 196(3), 197-212.

Fan, Q.C., Hooper, P.R., 1991. The Cenozoic Basaltic Rocks of Eastern China - Petrology and Chemical-Composition. Journal of Petrology, 32(4): 765-810.

Gao, S. et al., 1998. How mafic is the lower continental crust? Earth and Planetary

Always consult and cite the final, published document. See http:/www.minsocam.org or GeoscienceWorld

This is the peer-reviewed, final accepted version for American Mineralogist, published by the Mineralogical Society of America.
The published version is subject to change. Cite as Authors (Year) Title. American Mineralogist, in press.
DOI: https://doi.org/10.2138/am-2022-8254. http://www.minsocam.org/

612 Science Letters, 161(1-4): 101-117.

613 Ginibre, C., Davidson, J.P., 2014. Sr Isotope Zoning in Plagioclase from Parinacota
614 Volcano (Northern Chile): Quantifying Magma Mixing and Crustal
615 Contamination. Journal of Petrology, 55(6): 1203-1238.

616 Glazner, A.F., Farmer, G.L., 1992. Production of Isotopic Variability in Continental
617 Basalts by Cryptic Crustal Contamination. Science, 255(5040): 72-74.

618 Glazner, A.F., Farmer, G.L., Hughes, W.T., Wooden, J.L., Pickthorn, W., 1991.
619 Contamination of basaltic magma by mafic crust at Amboy and Pisgah Craters,
620 Mojave Desert, California. Journal of Geophysical Research: Solid Earth,
621 96(B8): 13673-13691.

622 Guo, P. et al., 2016. The origin of Cenozoic basalts from central Inner Mongolia, East
623 China: The consequence of recent mantle metasomatism genetically associated
624 with seismically observed paleo-Pacific slab in the mantle transition zone.
625 Lithos, 240–243: 104-118.

626 Hagen-Peter, G., Tegner, C., Lesher, C.E., 2019. Strontium isotope systematics for
627 plagioclase of the Skaergaard intrusion (East Greenland): A window to crustal
628 assimilation, differentiation, and magma dynamics. Geology, 47(4): 313-316.

629 Ho, K.S., Liu, Y., Chen, J.C., You, C.F., Yang, H.J., 2011. Geochemical
630 Characteristics of Cenozoic Jining Basalts of the Western North China Craton:
631 Evidence for the Role of the Lower Crust, Lithosphere, and Asthenosphere in
632 Petrogenesis. Terrestrial Atmospheric and Oceanic Sciences, 22(1): 15-40.

633 Hofmann, A.W. (1997) Mantle geochemistry: The message from oceanic volcanism.

Always consult and cite the final, published document. See http:/www.minsocam.org or GeoscienceWorld

This is the peer-reviewed, final accepted version for American Mineralogist, published by the Mineralogical Society of America.
The published version is subject to change. Cite as Authors (Year) Title. American Mineralogist, in press.
DOI: https://doi.org/10.2138/am-2022-8254. http://www.minsocam.org/

Nature, 385(6613), 218-229.

Huang, X.L., Xu, Y.G., Liu, D.Y., 2004. Geochronology, petrology and geochemistry of the granulite xenoliths from Nushan, east China: Implication for a heterogeneous lower crust beneath the Sino-Korean Craton. Geochimica Et Cosmochimica Acta, 68(1): 127-149.

Jiang, L., Zhi, X., 2010. Re-Os isotope geochemistry of basalts from Hannuoba, North China: Evidence for Re volatile loss and crust-mantle interaction. Acta Petrologica Sinica, 26(4): 1265-1276.

Jiang, N., Guo, J.H., Chang, G.H., 2013. Nature and evolution of the lower crust in the eastern North China craton: A review. Earth-Science Reviews, 122: 1-9.

Jochum, K.P. et al., 2011. Determination of Reference Values for NIST SRM 610-617 Glasses Following ISO Guidelines. Geostandards and Geoanalytical Research, 35(4): 397-429.

Jochum, K.P., Willbold, M., Raczek, I., Stoll, B., Herwig, K., 2005. Chemical characterisation of the USGS reference glasses GSA-1G, GSC-1G, GSD-1G, GSE-1G, BCR-2G, BHVO-2G and BIR-1G using EPMA, ID-TIMS, ID-ICP-MS and LA-ICP-MS. Geostandards and Geoanalytical Research, 29(3): 285-302.

Lange, A.E., Nielsen, R.L., Tepley, F.J., Kent, A.J.R., 2013. Diverse Sr isotope signatures preserved in mid-oceanic-ridge basalt plagioclase. Geology, 41(2): 279-282.

Li, C. et al., 2018. In-situ Sr isotopic measurement of scheelite using

Always consult and cite the final, published document. See http:/www.minsocam.org or GeoscienceWorld

This is the peer-reviewed, final accepted version for American Mineralogist, published by the Mineralogical Society of America.
The published version is subject to change. Cite as Authors (Year) Title. American Mineralogist, in press.
DOI: https://doi.org/10.2138/am-2022-8254. http://www.minsocam.org/

fs-LA-MC-ICPMS. Journal of Asian Earth Sciences, 160: 38-47.

Liu, C.Q., Masuda, A., Xie, G.H., 1994. Major-Element and Trace-Element Compositions of Cenozoic Basalts in Eastern China - Petrogenesis and Mantle Source. Chemical Geology, 114(1-2): 19-42.

Liu, J.A., Cai, R.H., Pearson, D.G., Scott, J.M., 2019. Thinning and destruction of the lithospheric mantle root beneath the North China Craton: A review. Earth-Science Reviews, 196.

Liu, Y., Zong, K., Kelemen, P.B., Gao, S., 2008a. Geochemistry and magmatic history of eclogites and ultramafic rocks from the Chinese continental scientific drill hole: Subduction and ultrahigh-pressure metamorphism of lower crustal cumulates. Chemical Geology, 247(1): 133-153.

Liu, Y.S., Gao, S., Kelemen, P.B., Xu, W.L., 2008b. Recycled crust controls contrasting source compositions of Mesozoic and Cenozoic basalts in the North China Craton. Geochimica Et Cosmochimica Acta, 72(9): 2349-2376.

Liu, Y.S. et al., 2004. U-Pb zircon ages and Nd, Sr, and Pb isotopes of lower crustal xenoliths from North China Craton: insights on evolution of lower continental crust. Chemical Geology, 211(1-2): 87-109.

Lustrino, M., 2005. How the delamination and detachment of lower crust can influence basaltic magmatism. Earth-Science Reviews, 72(1-2): 21-38.

McDonough, W.F., Sun, S.s., 1995. The composition of the Earth. Chemical Geology, 120(3–4): 223-253.

Neave, D.A., Putirka, K.D., 2017. A new clinopyroxene-liquid barometer, and

Always consult and cite the final, published document. See http:/www.minsocam.org or GeoscienceWorld

This is the peer-reviewed, final accepted version for American Mineralogist, published by the Mineralogical Society of America.
The published version is subject to change. Cite as Authors (Year) Title. American Mineralogist, in press.
DOI: https://doi.org/10.2138/am-2022-8254. http://www.minsocam.org/

implications for magma storage pressures under Icelandic rift zones. American Mineralogist, 102(4): 777-794.

Paton, C., Hellstrom, J., Paul, B., Woodhead, J., Hergt, J., 2011. Iolite: Freeware for the visualisation and processing of mass spectrometric data. Journal of Analytical Atomic Spectrometry, 26(12): 2508-2518.

Putirka, K.D., 2008. Thermometers and barometers for volcanic systems. Reviews in Mineralogy and Geochemistry, 69(1): 61-120.

Qian, S.-P., Ren, Z.-Y., Zhang, L., Hong, L.-B., Liu, J.-Q., 2015. Chemical and Pb isotope composition of olivine-hosted melt inclusions from the Hannuoba basalts, North China Craton: Implications for petrogenesis and mantle source. Chemical Geology, 401(0): 111-125.

Ramos, F.C., Reid, M.R., 2005. Distinguishing melting of heterogeneous mantle sources from crustal contamination: Insights from Sr isotopes at the phenocryst scale, Pisgah Crater, California. Journal of Petrology, 46(5): 999-1012.

Ramos, F.C., Wolff, J.A., Tollstrup, D.L., 2004. Measuring Sr-87/Sr-86 variations in minerals and groundmass from basalts using LA-MC-ICPMS. Chemical Geology, 211(1-2): 135-158.

Ramos, F.C., Wolff, J.A., Tollstrup, D.L., 2005. Sr isotope disequilibrium in Columbia River flood basalts: Evidence for rapid shallow-level open-system processes. Geology, 33(6): 457-460.

Rudnick, R.L., Fountain, D.M., 1995. Nature and Composition of the

Always consult and cite the final, published document. See http:/www.minsocam.org or GeoscienceWorld

This is the peer-reviewed, final accepted version for American Mineralogist, published by the Mineralogical Society of America.
The published version is subject to change. Cite as Authors (Year) Title. American Mineralogist, in press.
DOI: https://doi.org/10.2138/am-2022-8254. http://www.minsocam.org/

Continental-Crust - a Lower Crustal Perspective. Reviews of Geophysics, 33(3): 267-309.

Song, Y., Frey, F.A., Zhi, X.C., 1990. Isotopic Characteristics of Hannuoba Basalts, Eastern China - Implications for Their Petrogenesis and the Composition of Subcontinental Mantle. Chemical Geology, 88(1-2): 35-52.

Sun, C., Liang, Y., 2017. A REE-in-plagioclase–clinopyroxene thermometer for crustal rocks. Contributions to Mineralogy and Petrology, 172(4): 24.

Sun, C., Lissenberg, C.J., 2018. Formation of fast-spreading lower oceanic crust as revealed by a new Mg–REE coupled geospeedometer. Earth and Planetary Science Letters, 487: 165-178.

Tepley, I.F.J., Davidson, J.P., Tilling, R.I., Arth, J.G., 2000. Magma Mixing, Recharge and Eruption Histories Recorded in Plagioclase Phenocrysts from El Chichón Volcano, Mexico. Journal of Petrology, 41(9): 1397-1411.

Xu, R. et al., 2017. Crust recycling induced compositional-temporal-spatial variations of Cenozoic basalts in the Trans-North China Orogen. Lithos, 274–275: 383-396.

Xu, Y.G., Ma, J.L., Frey, F.A., Feigenson, M.D., Liu, J.F., 2005. Role of lithosphere-asthenosphere interaction in the genesis of Quaternary alkali and tholeiitic basalts from Datong, western North China Craton. Chemical Geology, 224(4): 247-271.

Yan, L.L., He, Z.Y., Xu, X.S., 2020. Magma recharge processes of the Yandangshan volcanic-plutonic caldera complex in the coastal SE China: Constraint from

Always consult and cite the final, published document. See http:/www.minsocam.org or GeoscienceWorld

This is the peer-reviewed, final accepted version for American Mineralogist, published by the Mineralogical Society of America.
The published version is subject to change. Cite as Authors (Year) Title. American Mineralogist, in press.
DOI: https://doi.org/10.2138/am-2022-8254. http://www.minsocam.org/

722 inter-grain variation of Sr isotope of plagioclase. Journal of Asian Earth
723 Sciences, 201.
724 Yang, Y.H. et al., 2014. Sr and Nd isotopic compositions of apatite reference materials
725 used in U-Th-Pb geochronology. Chemical Geology, 385: 35-55.
726 Yang, Z.-F., Li, J., Liang, W.-F., Luo, Z.-H., 2016. On the chemical markers of
727 pyroxenite contributions in continental basalts in Eastern China: Implications
728 for source lithology and the origin of basalts. Earth-Science Reviews, 157:
729 18-31.
730 Yang, Z.-F., Zhou, J.-H., 2013. Can we identify source lithology of basalt? Sci. Rep.,
731 3, 1856.
732 Zeng, G., Chen, L.H., Hofmann, A.W., Jiang, S.Y., Xu, X.S., 2011. Crust recycling in
733 the sources of two parallel volcanic chains in Shandong, North China. Earth
734 and Planetary Science Letters, 302(3-4): 359-368.
735 Zhang, L.L. et al., 2019. Late Cretaceous volcanic rocks in the Sangri area, southern
736 Lhasa Terrane, Tibet: Evidence for oceanic ridge subduction. Lithos, 326:
737 144-157.
738 Zhao, G.C., Wilde, S.A., Cawood, P.A., Sun, M., 2001. Archean blocks and their
739 boundaries in the North China Craton: lithological, geochemical, structural
740 and P-T path constraints and tectonic evolution. Precambrian Research,
741 107(1-2): 45-73.
742 Zhi, X., Song, Y., Frey, F.A., Feng, J., Zhai, M., 1990. Geochemistry of Hannuoba
743 basalts, eastern China: Constraints on the origin of continental alkalic and

Always consult and cite the final, published document. See http:/www.minsocam.org or GeoscienceWorld

This is the peer-reviewed, final accepted version for American Mineralogist, published by the Mineralogical Society of America.
The published version is subject to change. Cite as Authors (Year) Title. American Mineralogist, in press.
DOI: https://doi.org/10.2138/am-2022-8254. http://www.minsocam.org/

744 tholeiitic basalt. Chemical Geology, 88(1-2): 1-33.

745 Zou, H., 2000. Modeling of trace element fractionation during non-modal dynamic
746 melting with linear variations in mineral/melt distribution coefficients.
747 Geochimica Et Cosmochimica Acta, 64(6): 1095-1102.

748 **Figures**

749

Figure 1

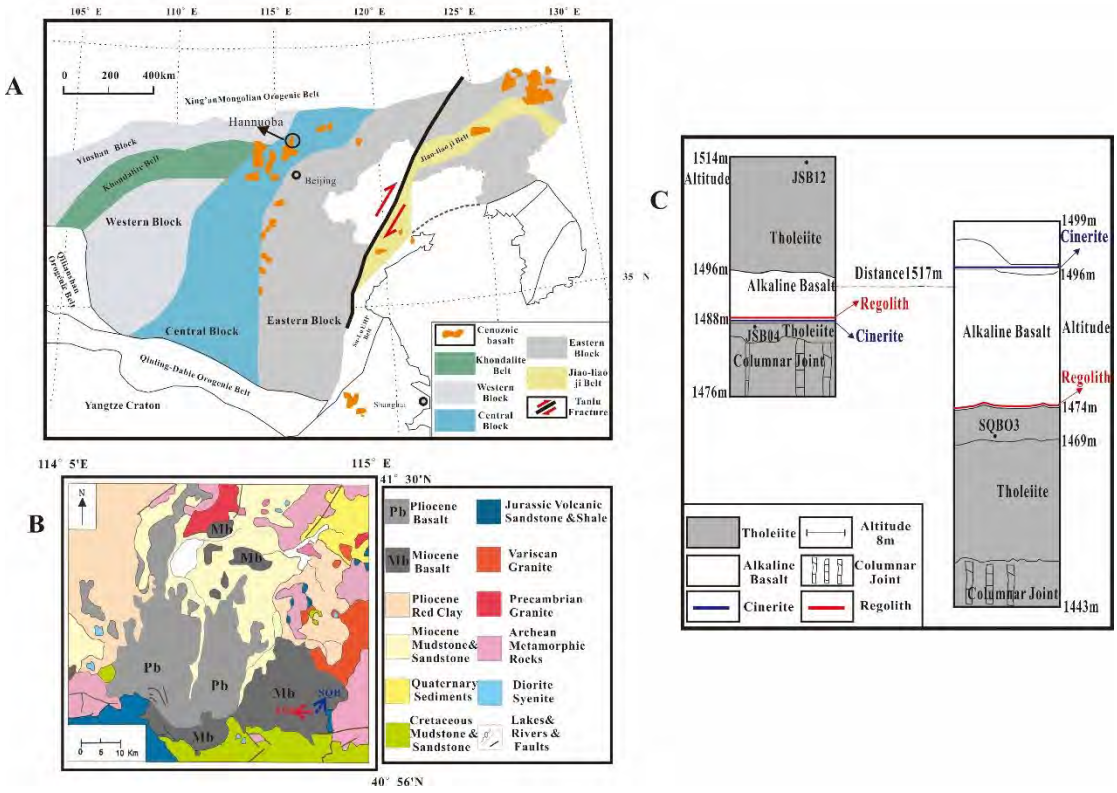

750

751 **Figure 1.** (a). Sketch map of the North China Craton（modified according to (Liu
752 et al., 2019; Xu et al., 2005) (b). Geological map of Hannuoba（modified according to
753 (Zhi et al., 1990) (c). Spatial distribution of basalt in the sampling area.

754

755

Always consult and cite the final, published document. See http:/www.minsocam.org or GeoscienceWorld

This is the peer-reviewed, final accepted version for American Mineralogist, published by the Mineralogical Society of America.
The published version is subject to change. Cite as Authors (Year) Title. American Mineralogist, in press.
DOI: https://doi.org/10.2138/am-2022-8254. http://www.minsocam.org/

Figure 2

Figure 2. Representative micro-textural characteristics of the Hannuoba tholeiite under crossed polars

Figure 3

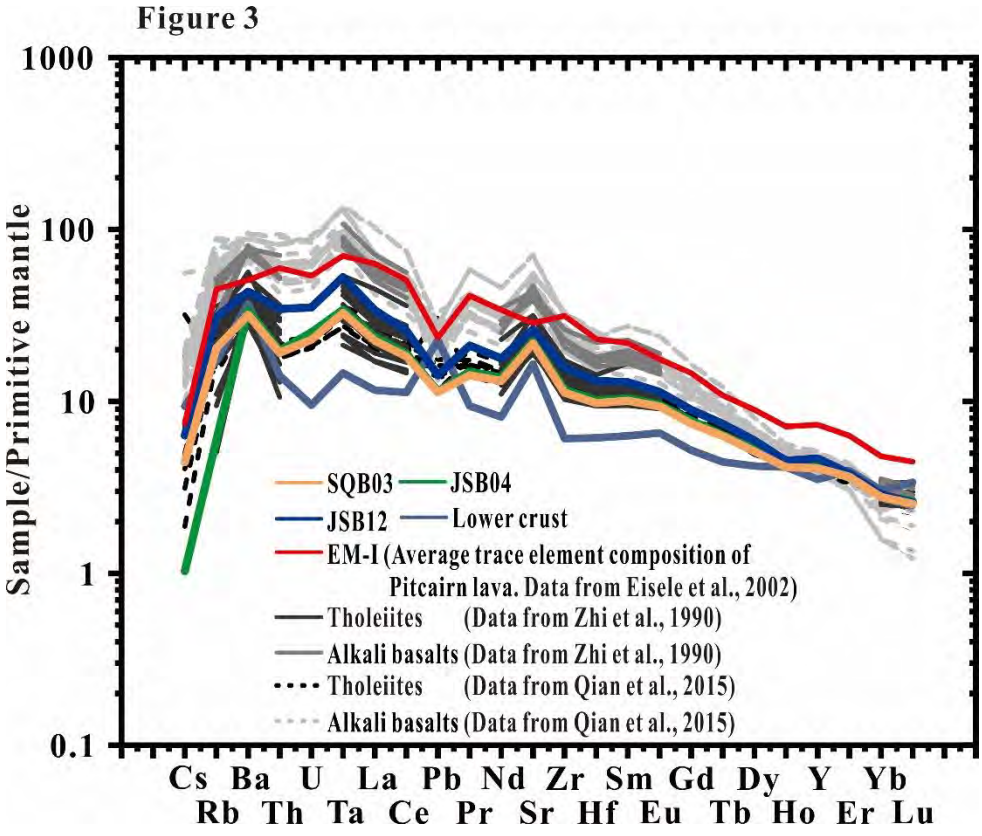

Figure 3. Primitive mantle (McDonough and Sun, 1995) normalized trace

Always consult and cite the final, published document. See http:/www.minsocam.org or GeoscienceWorld

This is the peer-reviewed, final accepted version for American Mineralogist, published by the Mineralogical Society of America.
The published version is subject to change. Cite as Authors (Year) Title. American Mineralogist, in press.
DOI: https://doi.org/10.2138/am-2022-8254. http://www.minsocam.org/

762 element pattern for Hannuoba basalts and the average lower continental crust.

763

Figure 4

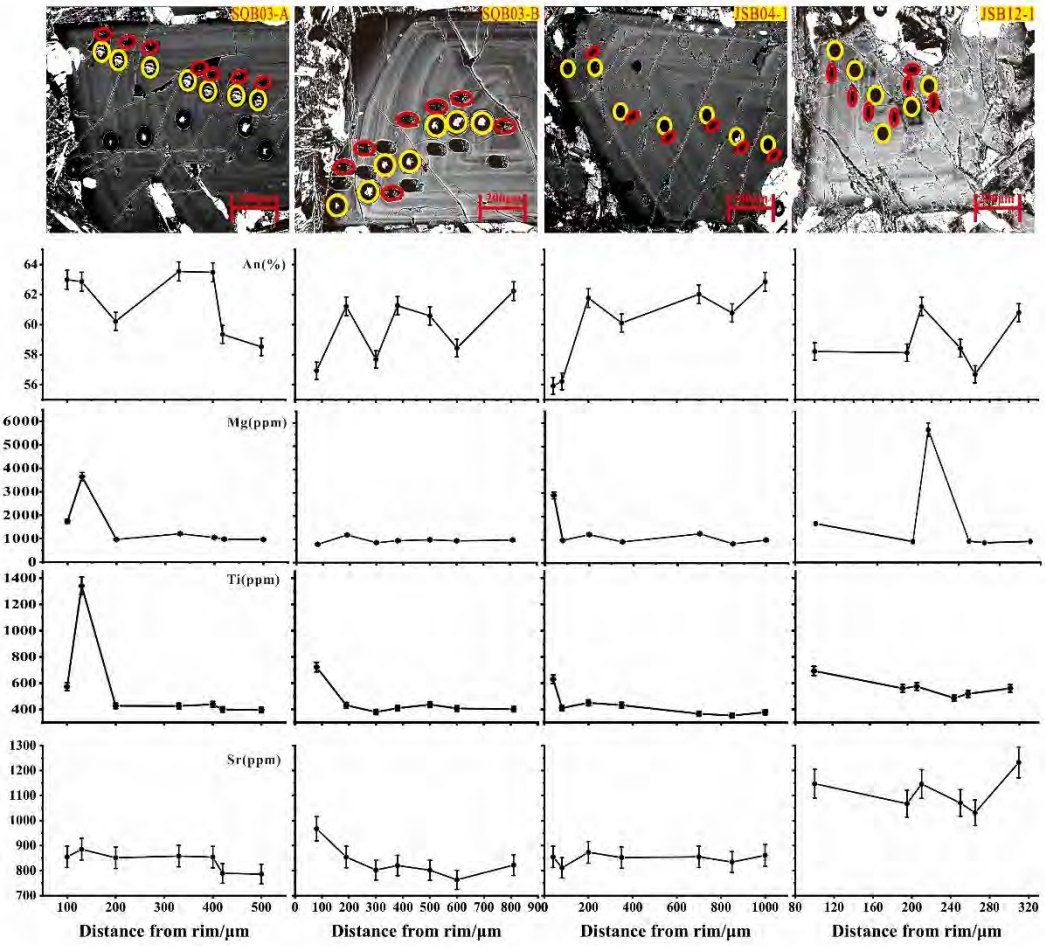

764

765 **Figure 4**. The relationship between An value and Mg, Ti, Sr element. (The

766 circles in yellow represent the in-situ trace element analyses, and the circles in red

767 represent the in-situ strontium isotope analyses. Error bars are 2σ SE)

Always consult and cite the final, published document. See http:/www.minsocam.org or GeoscienceWorld

This is the peer-reviewed, final accepted version for American Mineralogist, published by the Mineralogical Society of America.
The published version is subject to change. Cite as Authors (Year) Title. American Mineralogist, in press.
DOI: https://doi.org/10.2138/am-2022-8254. http://www.minsocam.org/

Figure 5

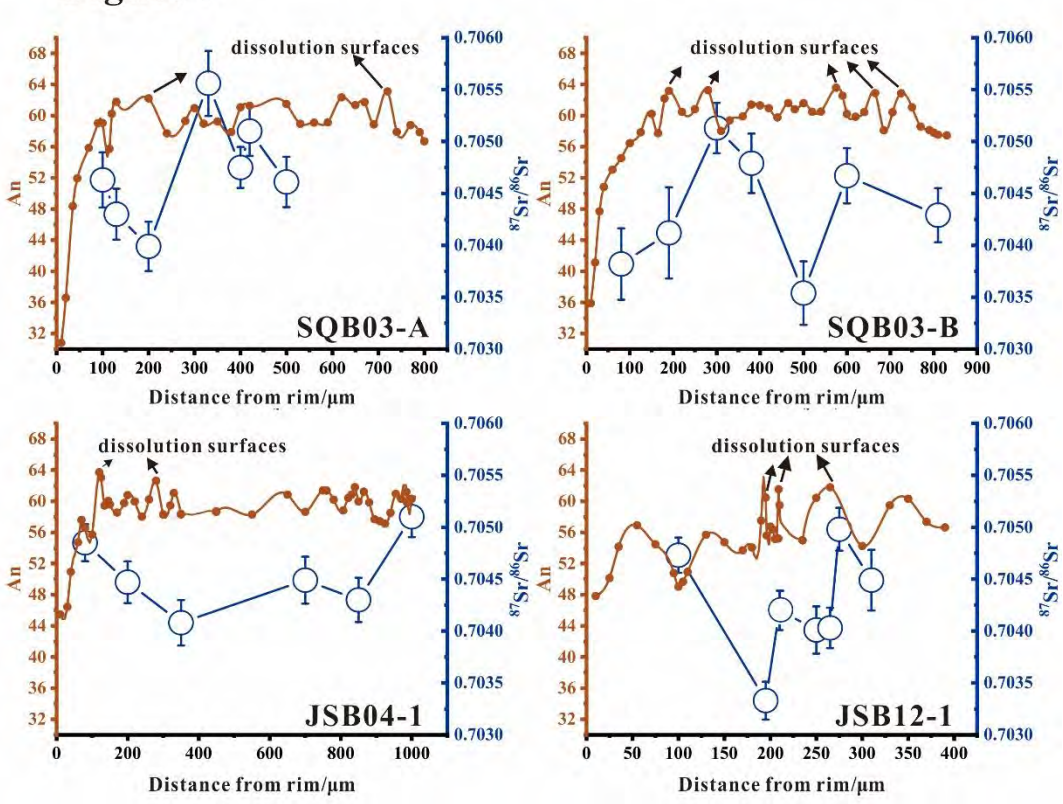

768

769 **Figure 5.** Variation diagram of Sr isotope, An, and distance in plagioclase.

770 The arrow indicates dissolution surfaces and major Sr isotope variation trends.

771 Error bars are 2σ SE.

772

Always consult and cite the final, published document. See http:/www.minsocam.org or GeoscienceWorld

This is the peer-reviewed, final accepted version for American Mineralogist, published by the Mineralogical Society of America.
The published version is subject to change. Cite as Authors (Year) Title. American Mineralogist, in press.
DOI: https://doi.org/10.2138/am-2022-8254. http://www.minsocam.org/

Figure 6

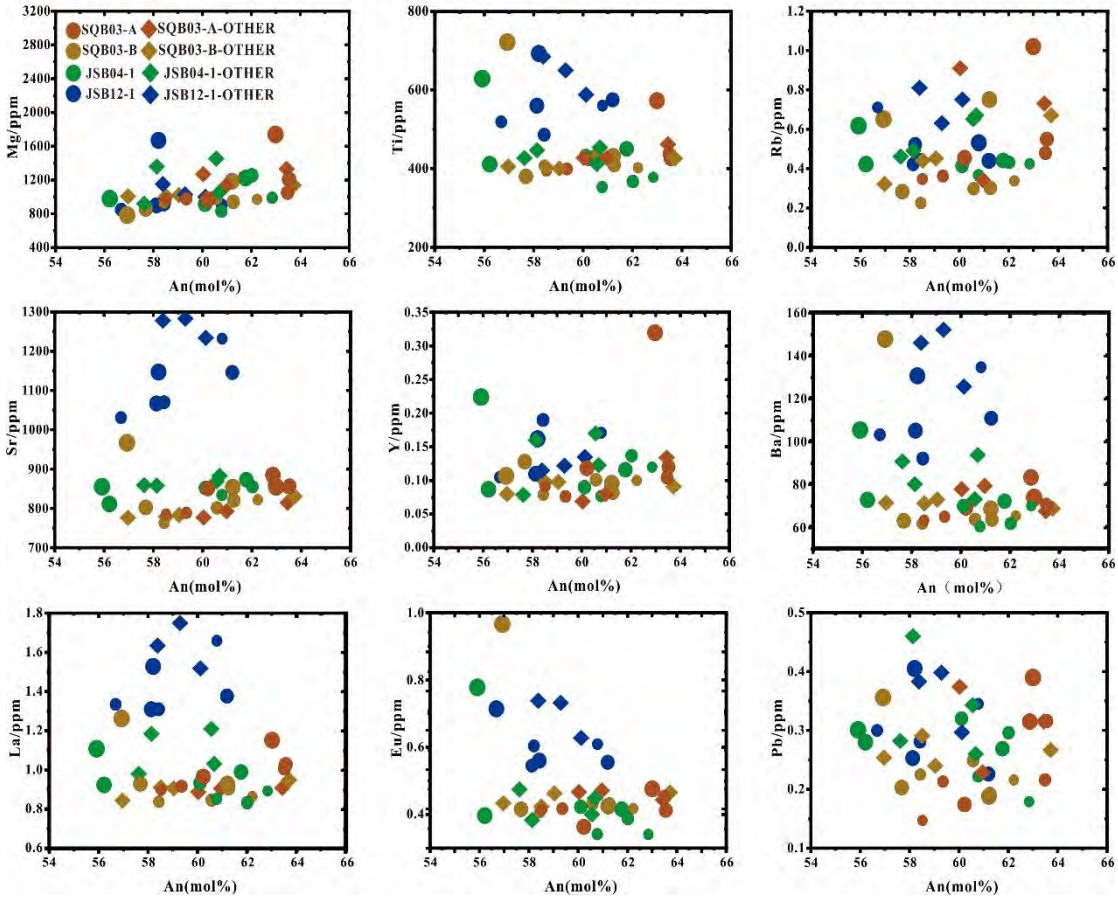

Figure 6. Relationship between trace element concentration and An content in plagioclase. The circle data measured isotopes simultaneously, and the diamond data are other plagioclase crystals randomly selected from each sample. Colored circles from large to small represent from rim to core.

Always consult and cite the final, published document. See http:/www.minsocam.org or GeoscienceWorld

This is the peer-reviewed, final accepted version for American Mineralogist, published by the Mineralogical Society of America.
The published version is subject to change. Cite as Authors (Year) Title. American Mineralogist, in press.
DOI: https://doi.org/10.2138/am-2022-8254. http://www.minsocam.org/

Figure 7

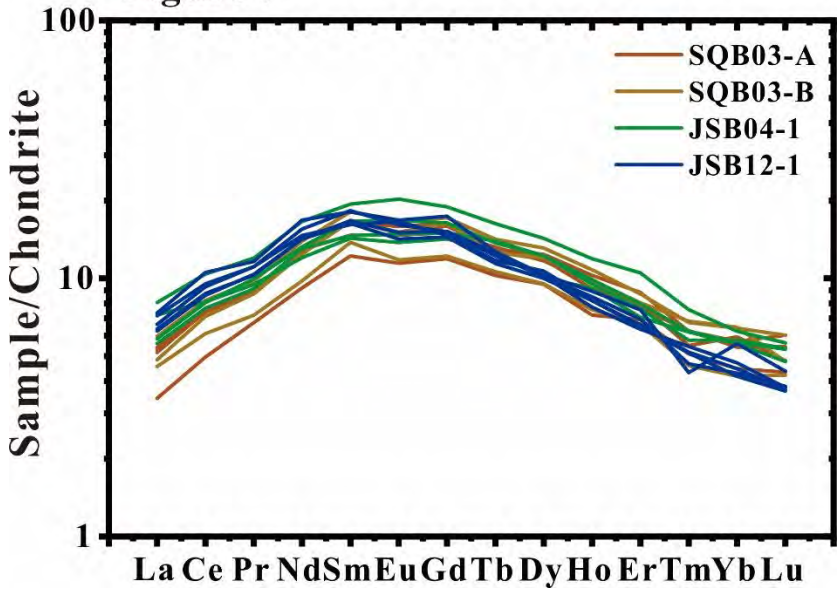

778

779 **Figure 7.** Chondrite-normalized (McDonough and Sun, 1995) REE

780 concentration patterns for clinopyroxenes from Hannuoba tholeiite

781

Figure 8

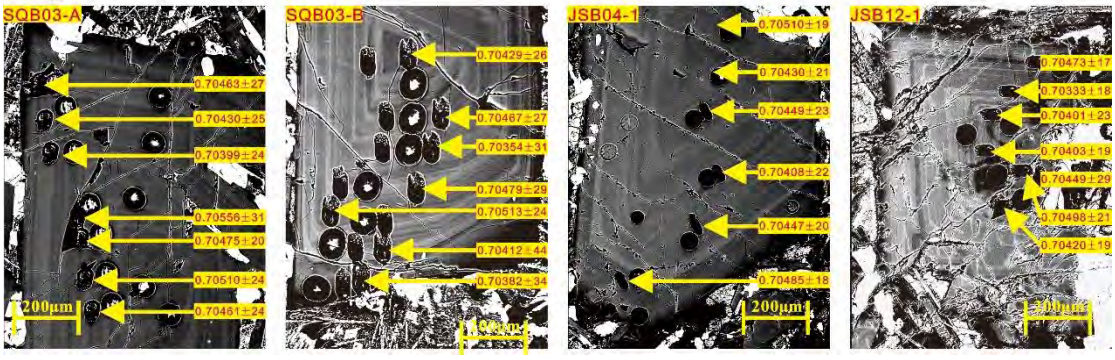

782

783 **Figure 8.** BSE image of the plagioclase sample with strontium isotope indicated.

784

Always consult and cite the final, published document. See http:/www.minsocam.org or GeoscienceWorld

This is the peer-reviewed, final accepted version for American Mineralogist, published by the Mineralogical Society of America.
The published version is subject to change. Cite as Authors (Year) Title. American Mineralogist, in press.
DOI: https://doi.org/10.2138/am-2022-8254. http://www.minsocam.org/

Figure 9

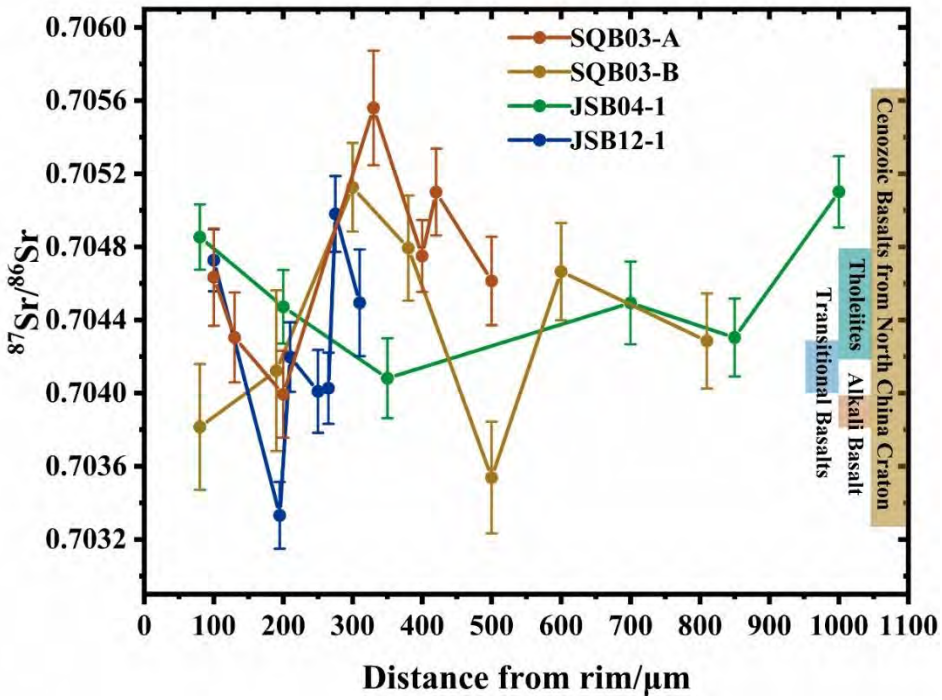

785

786 **Figure 9.** In situ $^{87}Sr/^{86}Sr$ variations of plagioclase samples from Hannuoba

787 basalts. Sr isotope data of whole-rock Hannuoba alkaline, transitional and tholeiitic

788 basalts are from (Song et al., 1990); Cenozoic basalts from North China Craton after

789 (Liu et al., 2008b). The error bar indicates 2σ SE.

790

Always consult and cite the final, published document. See http:/www.minsocam.org or GeoscienceWorld

This is the peer-reviewed, final accepted version for American Mineralogist, published by the Mineralogical Society of America.
The published version is subject to change. Cite as Authors (Year) Title. American Mineralogist, in press.
DOI: https://doi.org/10.2138/am-2022-8254. http://www.minsocam.org/

Figure 10

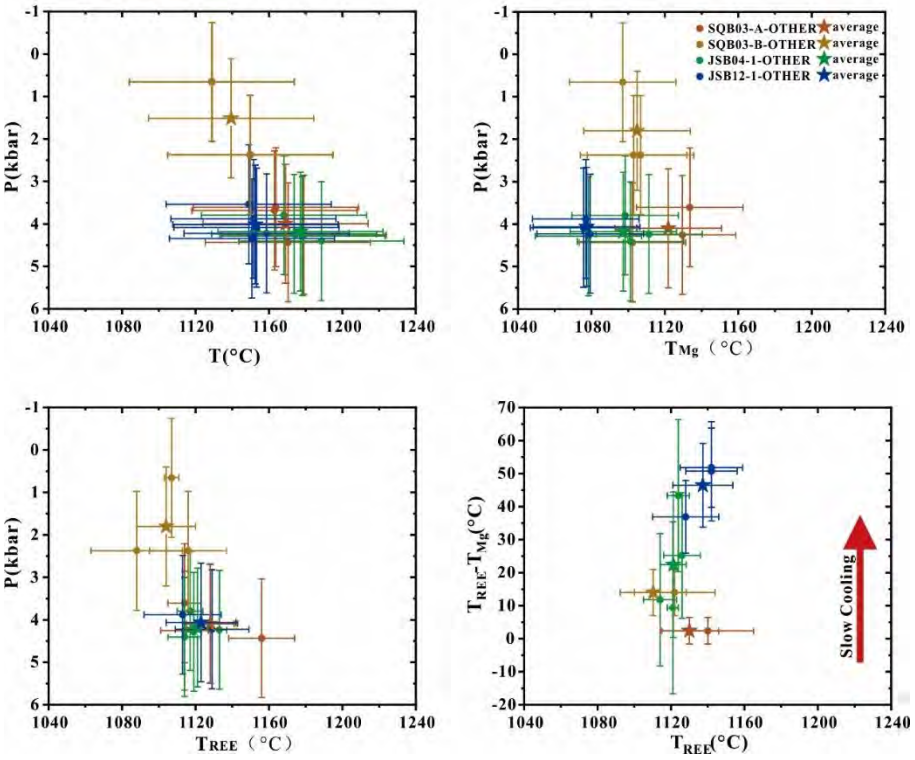

791

792 **Figure 10**. Relationship between crystallization temperature and pressure of

793 tholeiite in Hannuoba. (a) Crystallization pressure and temperature of clinopyroxene–

794 melt. (b) Closure temperature obtained by pyroxene-plagioclase magnesium

795 thermometer. (c) Closure the temperature obtained by pyroxene-plagioclase trace

796 element thermometer. (d) The temperature difference between T_{Mg} and T_{REE}. The error

797 bar indicates 2σ SE.

798

Always consult and cite the final, published document. See http:/www.minsocam.org or GeoscienceWorld

This is the peer-reviewed, final accepted version for American Mineralogist, published by the Mineralogical Society of America.
The published version is subject to change. Cite as Authors (Year) Title. American Mineralogist, in press.
DOI: https://doi.org/10.2138/am-2022-8254. http://www.minsocam.org/

Figure 11

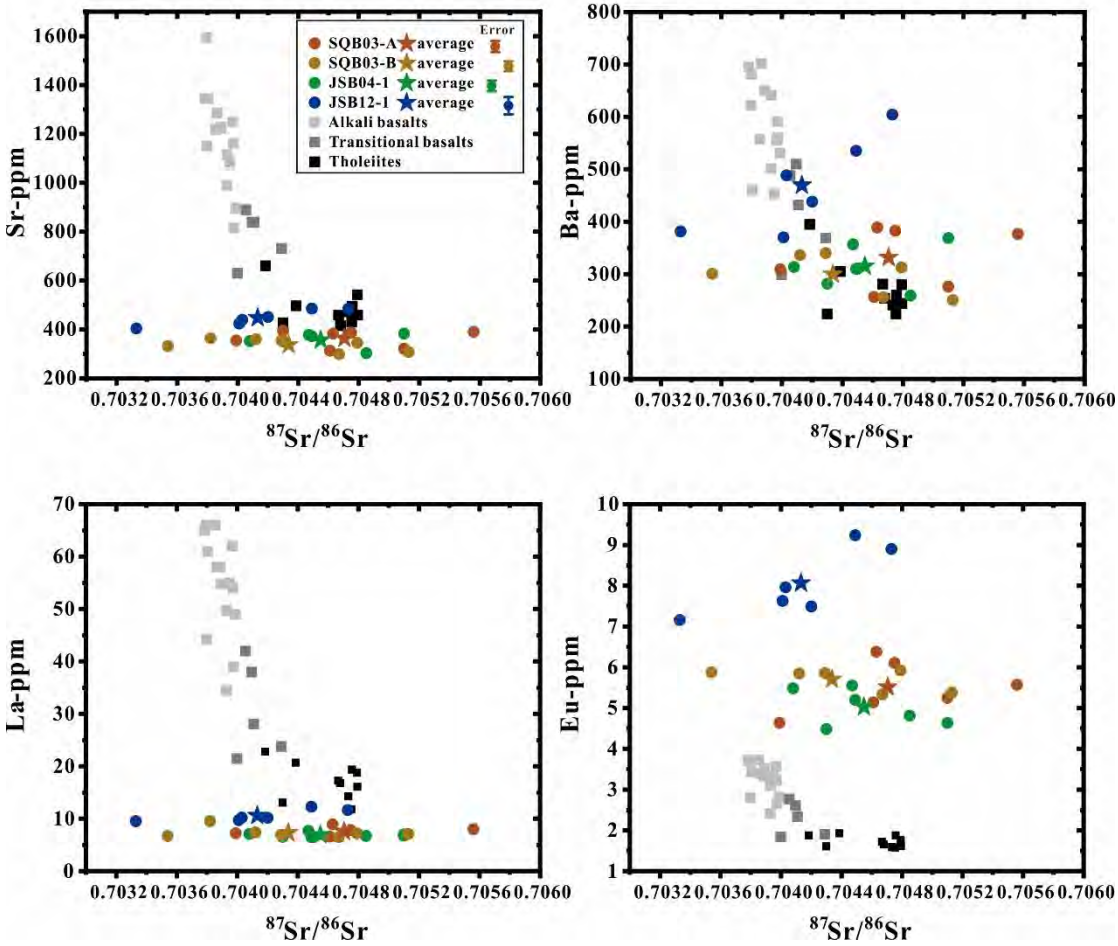

Figure 11. Sr isotope versus trace element content for Hannuoba basalts and the calculated melts in equilibrium with plagioclase**.** Hannuoba basalts from Zhi et al., 1990; Song et al., 1990. Error bars smaller than the symbol are not shown.

Always consult and cite the final, published document. See http:/www.minsocam.org or GeoscienceWorld